MULTIPARAMETRIC TRAVELTIME INVERSION

Ricardo Biloti, Lúcio T. Santos, and Martin Tygel

*State University of Campinas, Institute of Mathematics, Statistics, and Scientific Computing, Department of Applied Mathematics, Campinas–SP, Brazil**

Received: 11 November 2001; *Accepted: 25 February 2002.*

Abstract

In conventional seismic processing, the classical algorithm of Hubral and Krey is routinely applied to extract an initial macrovelocity model that consists of a stack of homogeneous layers bounded by curved interfaces. Input for the algorithm are identified primary reflections together with normal moveout (NMO) velocities, as derived from a previous velocity analysis conducted on common midpoint (CMP) data. This work presents a modified version of the Hubral and Krey algorithm that is designed to extend the original version in two ways, namely (a) it makes an advantageous use of previously obtained common-reflection-surface (CRS) attributes as its input and (b) it also allows for gradient layer velocities in depth. A new strategy to recover interfaces as optimized cubic splines is also proposed. Some synthetic examples are provided to illustrate and explain the implementation of the method.

Keywords: CRS, hyperbolic traveltime, macrovelocity inversion

1 Introduction

The CRS stacking method (see, e.g., Müller et al. (1998)) is a recent technique that is establishing itself as a better alternative to the conventional NMO/DMO stacking. As recently shown in Trappe et al. (2001) (see also more references therein), the CRS stack is able to provide, in a number of cases, significantly improved stacked sections that represent simulated zero-offset sections. The CRS stacking method provides, in addition to a better stacking, a set of parameters (called the CRS attributes) that convey more information of the propagating medium than the single parameter, the NMO-velocity, that results from the NMO/DMO stack. The CRS attributes are obtained by means of coherence analysis directly performed on the multicoverage data (see, e.g., Birgin et al. (1999)). The present paper is concerned with the use of CRS attributes for velocity model inversion.

One of the important aims of seismic processing is the construction of a depth velocity model that is consistent with the traveltimes of previously identified primary reflections. In this sense, the classical algorithm of Hubral and Krey (1980), is routinely used to produce a layered homogeneous velocity model that makes use of NMO analysis of CMP data. The natural question is, can the additional

*P.O. Box 6065, 13081-970, Campinas–SP, Brazil (e-mail: biloti@ime.unicamp.br).

information provided by the CRS attributes, that naturally result from the application of the CRS stacking, be advantageously used for model inversion purposes?

Following earlier publications (Berkovitch and Gelchinsky (1989), Berkovitch et al. (1991), Majer (2000) and Vieth (2001)), we provide a positive answer to that question. As shown below (see also Biloti et al. (2001) and Biloti (2001)), we can readily adapt the Hubral and Krey algorithm to use the CRS attributes, that naturally result from the application of the CRS stacking method to the given multicoverage data, so as to also obtain a layered model that is consistent with identified reflections. Because of the cleaner sections that result from the CRS stack, the input reflections tend to be easier to identify and select, leading to a more stable and reliable procedure.

The proposed method leads to consistent velocity models in a simple and fast manner. As a consequence, the obtained velocity models can be regarded as inputs for further inversion procedures, such as seismic tomography.

An important feature of the proposed algorithm is that it allows for velocity gradients within the layers, thus enlarging the application possibilities for subsequent imaging procedures. Moreover, special schemes designed for keeping track of the correct selection of attributes in the presence of complicated regions, such as caustic triplications, guarantees the stable recovery of the interfaces that define the layer model.

Hyperbolic Traveltime and CRS parameters. For a given fixed, reference ray, the hyperbolic traveltime moveout expression (see, e.g., Schleicher et al. (1993); Tygel et al. (1997)), relates the (squared) traveltime of that ray with the (squared) traveltime of any other ray (of the same code) in its vicinity. The denominations *central ray* and *paraxial rays* are commonly employed to designate the reference and vicinity rays, respectively. The important property of the traveltime moveout expression under consideration is that it is completely given in terms of (a) the initial and end point relative positions of the paraxial rays with respect to the central ray and (b) the dynamic properties of the central ray only. The latter are specified by means of the so-called surface-to-surface propagator matrix of the central ray.

We consider the 2-D situation in which sources and receivers are located on a single seismic line. In the case where the central ray is a zero-offset ray at the central point X_0 (see Figure 1), the hyperbolic moveout formula reads

$$T^2(x,h) = \left(t_0 + \frac{2x\sin\beta_0}{v_0}\right)^2 + \frac{2t_0\cos^2\beta_0}{v_0}\left(K_N\, x^2 + K_{NIP}\, h^2\right). \qquad (1)$$

Here, x and h are the midpoint and half-offset coordinates of the source and receiver pair in the vicinity of the normal ray. More specifically,

$$x = (x_G + x_S)/2 - x_0 \quad \text{and} \quad h = (x_G - x_S)/2\,,$$

where x_S and x_G are the horizontal coordinates of the source and receiver pair (S,G) near X_0, which has horizontal coordinate x_0. Moreover, t_0 is the zero-offset traveltime at X_0 and β_0 is the angle of emergence of the zero-offset ray with respect to the surface normal at the central point X_0. The quantity K_{NIP} is the wavefront curvature that the normal-incident-point wave (NIP-wave) has when it hits the surface at point X_0. Analogously, K_N is the wavefront curvature that the normal wave

(N-wave) has when it hits the surface at point X_0. For further details about NIP- and N-wave, we refer the reader to Hubral (1983). The traveltime formula (1) is of fundamental importance in the CRS method. Therefore, those three parameters, β_0, K_N and K_{NIP} are called CRS parameters.

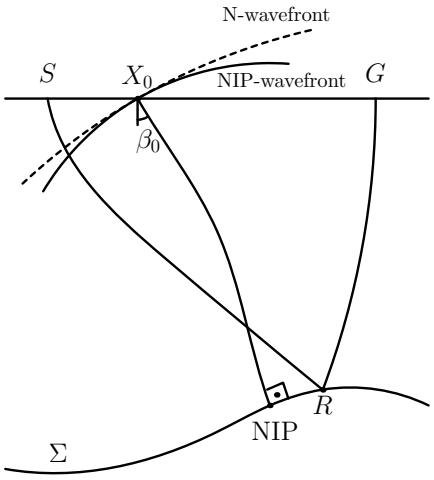

Figure 1: CRS Parameters for a normal central ray X_0 NIP X_0: the emergence angle β_0 and the NIP- and N-wavefront curvatures. Σ is the reflector, X_0 is the central point coordinate, and S and G are the source and receiver positions for a paraxial ray, reflecting at R.

2 Inversion of homogeneous layers

Our inversion method is based on the well-established algorithm described in Hubral and Krey (1980). There, the velocity model to be inverted from the data is assumed to consist of a stack of homogeneous layers bounded by smoothly curved interfaces. The unknowns are the velocity in each layer and the shape of each interface. These unknowns are iteratively obtained from top to bottom by means of a layer stripping process.

The main idea of the Hubral and Krey algorithm is to backpropagate the NIP-wave down to the NIP located at the bottom interface of the layer to be determined (see Figure 2). This means that the velocities and the reflectors above the layer under consideration have already been determined. Since the NIP-wave is due to a point source at the NIP, the backpropagation through this last layer gives us a focusing condition from which the unknown layer velocity can be determined. Note that we really need to backpropagate the NIP-wave through the ray path, since only for homogeneous media the center of curvature of the NIP-wave coincides with the NIP.

To determine the wavefront curvature along a ray path that propagates through the layered medium, Hubral and Krey (1980) combine two distinct situations: (a) the propagation occurs inside a homogeneous layer and (b) transmission occurs across an interface.

Figure 3 depicts a ray that traverses the j-th homogeneous layer (of velocity v_j) being transmitted (refracted) at the interface $j+1$. Let us denote by K_j^+ the wavefront curvature at the initial point of the ray (that is, just below the j-th interface). The wavefront curvature, K_{j+1}^-, just before transmission,

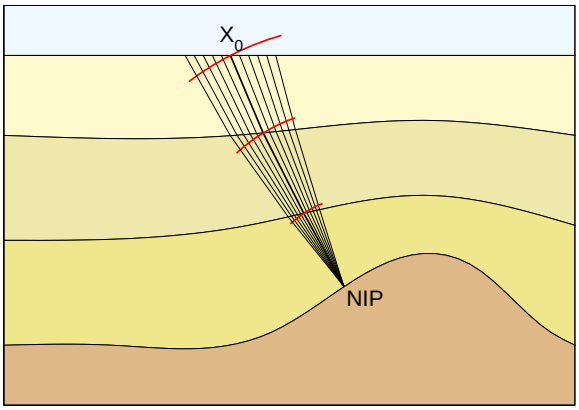

Figure 2: NIP-wavefront associated to the central zero-offset ray X_0 NIP X_0.

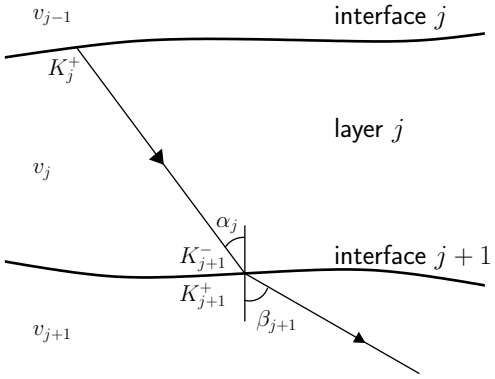

Figure 3: Ray propagation through homogeneous layer j.

satisfies the relationship

$$\frac{1}{K_{j+1}^-} = \frac{1}{K_j^+} + v_j \, \Delta t_j \ , \tag{2}$$

where Δt_j is the traveltime of the ray inside the layer. The change in wavefront curvature due to transmission at the interface, as also shown in Hubral and Krey (1980), is given by

$$K_{j+1}^+ = \frac{v_{j+1}}{v_j} \frac{\cos^2 \alpha_j}{\cos^2 \beta_{j+1}} K_{j+1}^- + \left(\frac{v_{j+1}}{v_j} \cos \alpha_j - \cos \beta_{j+1} \right) \frac{K_{j+1}^I}{\cos^2 \beta_{j+1}} \, , \tag{3}$$

where, α_j and β_{j+1} are the incident and transmission angles of the ray, respectively, and K_{j+1}^I is the curvature of the interface, all these quantities being measured at the transmission point. Observe that Snell's law,

$$\frac{\sin \alpha_j}{v_j} = \frac{\sin \beta_{j+1}}{v_{j+1}} \, , \tag{4}$$

is valid. Assume now that the NIP is located at the $(M+1)$-th interface. This leads to the *focusing conditions*

$$\frac{1}{K_{M+1}^-} = 0 = \frac{1}{K_M^+} + v_M \, \Delta t_M \quad \text{and} \quad \Delta t_M = t_0 - \left(\sum_{j=1}^{M-1} \Delta t_j \right) \, , \tag{5}$$

that determine the velocity v_M. Here, K_{M+1}^- is the wavefront curvature at the NIP (it starts as a point source) and K_M^+ is the wavefront curvature after transmission across the interface M. Note that K_M^+, as given by setting $j = M-1$ in equation (3), has an implicit dependence on v_M and β_M. This is because, by Snell's law,

$$\sin\beta_M = \frac{\sin\alpha_{M-1}}{v_{M-1}}\, v_M \ . \tag{6}$$

Once v_M and β_M were determined, the segment of the zero-offset ray inside the M-th layer can be constructed. The sought-for NIP location is then such that its distance to that transmission point is $v_M \Delta t_M$.

3 Hubral and Krey algorithm

It is instructive to discuss the key ideas involved in the preceding strategy. This is done below. We first present the main steps of the algorithm. Next we make some comments about the implementation of the various steps.

The method aims to extract a model composed by homogeneous layers separated by smoothly curved reflectors, corresponding to the well identified interfaces within the data only. This choice is made *a priori* by the user.

Determination of the first layer: The input data is, for each zero-offset ray, the traveltime t_0, the emergence angle β_0 and the wavefront curvature K_{NIP}. The velocity of the first layer is assumed to be known. Thus, only the reflector (the bottom of the first layer) should be determined. As explained below, this can be achieved in many different ways.

Determination of the jth-layer: Suppose that the model has been already determined up to the $(j-1)$th-layer. The method will proceed to the determination of the next layer, that is, the velocity of the jth-layer and the shape and location of the $(j+1)$th-interface. The input data is again, for each zero-offset ray reflecting at the interface $(j+1)$, the traveltime t_0, the emergence angle β_0 and the wavefront curvature K_{NIP}. Trace the zero-offset ray down to the j-th interface. Recall that this ray makes the angle β_0 with the surface normal at its initial point. Now, using equations (2) and (3), back-propagate the NIP-wave from the surface to the j-th interface along that ray. Finally, use the focusing conditions (5) to determine the layer velocity v_j, the angle β_j and the NIP.

The above procedure can, in principle, be done to each zero-offset ray. However, under the constraint that the layer velocity v_j is constant, we obtain an over-determined system of equations for that unknown. How to deal with this problem will be discussed below.

3.1 Brief discussion of the algorithm

We now comment on the above algorithm with regards to its accuracy and implementation. Our aim is to identify those aspects that can be improved upon the introduction of the CRS methodology.

- The quantities needed by the method (emergence angles, normal traveltimes and NIP-wavefront curvatures) are not directly available, but have to be extracted from the data. In the description in Hubral and Krey (1980), these quantities are obtained by conventional processing on CMP data.

- Note that the main idea of the method, the back-propagation of the NIP-wavefront, is carried out independently for each ray. Thus, in principle, each ray carries enough information to recover the layer velocity, that can be translated into many equations depending on the same unknown. Since we are assuming homogeneous layers, this implies an over-determination of the velocity. Of course, this question was faced on the original algorithm, but the methodology applied is not stated in the text. Hubral and Krey (1980) have pointed out that this "excess" of information could be used to improve the velocity distribution considered, for example, assuming a linear velocity variation.

- Note that the law of transmission for the wavefront curvatures depends on the curvature of the interface (K^I) at the transmission point, as we can see on formula (3). Hubral and Krey (1980) state that this can be obtained by a normal ray migration.

- The N-wavefront curvature, K_N, is not used in the original Hubral and Krey algorithm. This attribute, that relates to the curvature of the interface where the NIP is located, had not yet been introduced at the time the method was proposed.

- As stated in Hubral and Krey (1980), after the determination of the velocity, the location of each NIP can be obtained by down propagating the last ray segment. Since each ray hits the interface normally, the local dip can also be determined.

In the next section we show, with the help of the CRS attributes, how most of the difficulties addressed above can be solved. In this way, a more accurate and efficient version of the algorithm can be obtained and, moreover, preserving its elegant structure.

4 The revised Hubral and Krey algorithm

In this section we discuss how the CRS parameters can be used to fully supply the requirements of the Hubral and Krey algorithm and also how to address the involved numerical aspects. Then, we present a revised version of the original algorithm.

The obvious advantage of having the CRS parameters is that emergence angles and NIP-wavefront curvatures have been already determined. Moreover, due to the far more redundancy that is employed in the CRS stack, stacked sections are expected to be cleaner. This helps to a easier selection of the horizons of interest. Recent practical results in support of these considerations are reported in Trappe et al. (2001).

The CRS method also provides the N-wavefront curvatures, K_N, not used in the original Hubral and Krey algorithm. However, this parameter is the most unstable to estimate. Therefore, the incorporation of K_N in the inversion procedure should require special care. A possible use of K_N is the following: recall that the N-wave starts at the NIP, having the same curvature as the reflector.

After the determination of a given interface, we could back-propagate the N-wavefronts associated to this interface, applying the same procedure as described for the NIP-wavefront. Such a procedure would provide an estimate of the curvature of the reflector at the NIP. Note that this estimate is independent on how dense the NIPs are. Our tests showed that this scheme was too sensitive to errors in K_N, so it has not been adopted. As shown below, we have introduced a new reconstruction technique that simultaneously accounts for the shape and curvatures of the interfaces.

We now proceed to point out the main features of the proposed algorithm.

Smoothing. Special care is to be taken when using estimated quantities as input data. We have to try to avoid or, at least, reduce the effect of the estimation errors on the inversion process. The strategy applied in our implementation is to smooth the parameter curves. In the case of smooth interfaces, this makes good sense, since no abrupt variations on the parameters can in general occur. Although not tested, we expect the algorithm also to work under localized parameter discontinuities (such as encountered in faults and diffractors). This is because the inversion should correctly recover at least the smooth parts of the interfaces. The smoothing method used is stated in Leite (1998): For each five neighboring points on the curve, we fit a least-square parabola and replace the middle point by the corresponding one that belongs to the parabola (see Figure 4). This smoothing technique can be applied several times (we have used five times) to each parameter curve.

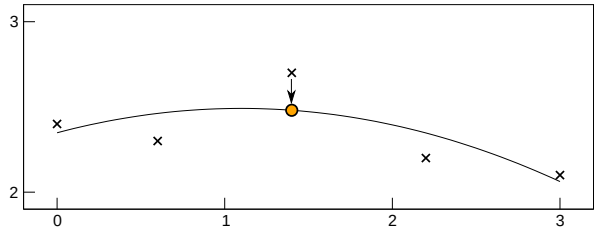

Figure 4: For each five points, the smoothing scheme fits a parabola and replaces the central point to its corresponding value at the parabola.

Unfolding criterion. The above-described smoothing method can be applied to any curve on the plane. All we need to know is how to follow the curve. In our case, the curves are parametrized by the central point coordinate. In caustic regions, more than one set of parameter values are associated to the same central point. This could generate a problem to find out the correct sequence. The reader could argue that perhaps the correct order is already known. However, since the CRS parameters are extracted from the parameter sections by some picking process, the method that we describe can be automatically built in the picking process. At the left side of Figure 5 we can see a situation where the parameter values are sorted by their central-point coordinates, and at the right side of the same figure we can see the case where the parameter values are correctly sorted.

We have formulated a criterion to unfold the parameter curve. When the curve has more than one value for the same central point coordinate, the proposed criterion tries to keep the variations of the CRS parameters between two neighboring points on the curve as small as possible. This is a reasonable assumption since a smooth behavior of the CRS parameters is expected. The merit function which is

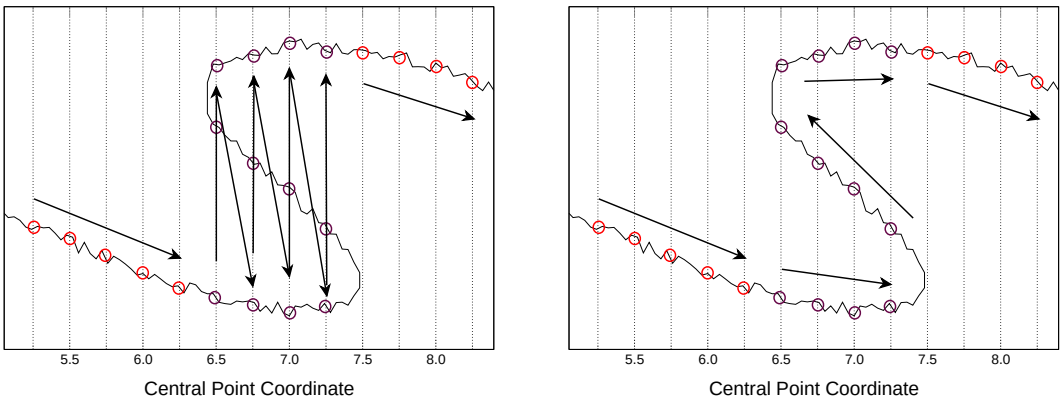

Figure 5: Both figures show a parameter curve within a caustic region. The small circles denote the sampled values of the parameter. At left, the points on the curve are sorted by their central-point coordinates. The arrows indicate the obtained sequence. At right, the same points were resorted to the correct sequence by the application of the unfolding criterion.

to be minimized is

$$F(\mathbf{p}_j, \mathbf{p}_i) = \frac{|t_0^j - t_0^i|}{t_0^i} + \frac{|\beta_0^j - \beta_0^i|}{|\beta_0^i|}\,. \tag{7}$$

Here, $\mathbf{p}_i = (t_0^i, \beta_0^i)$ is a vector with components t_0^i (traveltime) and β_0^i (emergence angle), that refer to the central-point coordinate, x_0^i. Also, i is the index of the current point and j varies on the set of indices that specify their associated neighboring points. We calculate the function above for each point in the vicinity of point i. Thereafter, we assign the point that has achieved the minimum value of F to be the next one in the reordered sequence. We observe that we made additional tests including, in the merit function F, two more terms, one for K_{NIP} and one for K_N. However, we got worse results concerning the stability of the scheme. Recall that the above unfolding criterion is to be applied before the smoothing process. So it should work even if there is noise in the obtained parameter values. Several tests have confirmed the ability of the proposed criterion to effectively unfold the parameter curve.

Model with vertical velocity gradients. As earlier described, the velocity determination is carried out at each normal ray, leading to an over determination problem. To approach the velocity over-determination, we consider a solution in the sense of least squares as described below.

Our proposed algorithm assumes that the layered velocity model to be constructed is such that the velocity, in each layer, has a constant gradient in depth z-direction (an affine function on the depth). In other words, the velocity of the jth-layer is

$$v_j(z) = a_j z + b_j\,, \tag{8}$$

with constant values of a_j and b_j. As previously indicated, this feature is a significant improvement of the original Hubral and Krey algorithm in the sense that the latter admits only constant-velocity layers. Use of more general velocity profiles as in equation (8), implies that the the formulas (2) and

(3), designed for homogeneous layers, are no longer valid. To account for variations of velocity inside the layers, we have used standard ray-theoretical results (see, e.g., Červený (2001)), to derive the corresponding expressions for propagation and transmission of wavefront curvatures in layered media with velocity as in (8). For the propagation of wavefront curvatures from a point A to a point B we found

$$K(B) = \frac{v(B)}{v(A)} \left(K(A)^{-1} + \frac{\sigma(B,A)}{v(A)} \right)^{-1} , \tag{9}$$

where

$$\sigma(B,A) = \frac{\operatorname{sign}(\cos\gamma)}{a p_0^2} \left(\sqrt{1 - p_0^2 v(A)^2} - \sqrt{1 - p_0^2 v(B)^2} \right) , \tag{10}$$

γ is the angle between the tangent of the ray at A and the vertical axis, a is the gradient of v, and p_0 is the ray parameter. The transmission law of curvatures across an interface is found to be

$$K^+ = \frac{v^+}{v^-} \left(\frac{\cos\alpha}{\cos\beta} \right)^2 K^- + \left(\frac{v^+}{v^-} \cos\alpha - \cos\beta \right) \frac{K^I}{\cos^2\beta} + \frac{2\cos\alpha(\sin\alpha)^2 \sin\gamma^- a^-}{v^-(z)} , \tag{11}$$

where a^- is the gradient of v^-, as in equation (8). The superscripts - and + account for the quantities before and after the transmission through the interface, respectively. The first term accounts for the wavefront deformation due to the transmission through the interface, in this sense it considers only the variations on the velocity along the normal of the surface. The second one accounts for the interference of the interface curvature. Finally, the third term of the equation (11) accounts for the heterogeneities on the velocity in the tangent direction to the surface. Thus, this last term vanishes for the case of layers with constant velocity.

Interface construction. Concerning the construction of the layer interfaces, our approach is to fit a cubic spline, in the sense of least squares, to the set of obtained NIPs. Remember that, after the determination of the layer velocity, each zero-offset ray can be propagate down to its correspondent NIP (see Figure 6). The optimization solver employed is the GENCAN, proposed by Birgin and Martínez

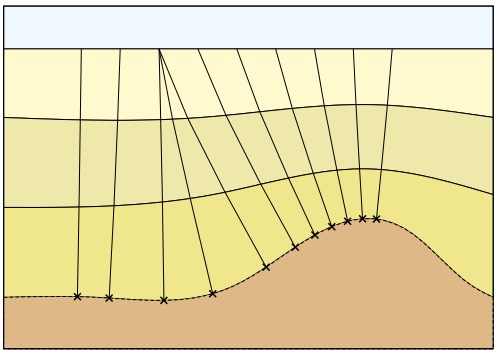

Figure 6: Several NIPs (crosses) obtained by propagation of the last ray segments.

(2001). GENCAN is an active-set method for smooth box-constrained minimization. The algorithm combines an unconstrained method, including a line-search which aims to add many constraints to the working set at a single iteration, with a recently introduced technique (spectral projected gradient) for dropping constraints from the working set.

5 Implementation of the revised Hubral and Krey algorithm

In the following, we present and comment our implementation scheme of the algorithm of revised Hubral and Krey as proposed in this work.

Input data. Recall that after the application of the CRS method, we obtain a simulated zero-offset section in which the events of interest (selected primary reflections) are well identified. This means that the traveltimes t_0 at each reflection can be easily picked. The identified primary reflections will provide the interfaces of the layered model to be inverted. Also recall that, attached to each point of the simulated zero-offset section, we have the three parameters β_0, K_{NIP} and K_N, that have been extracted from the multicoverage data. We finally note that the velocity of the medium in the vicinity of each central point is assumed to be *a priori* known.

Determination of the first layer. For a given central point X_0, let t_0 be the zero-offset traveltime of the primary reflection at the first interface. Also, let β_0 be the corresponding emergence angle. In the present form of the algorithm, we assume that the velocity of the first layer is known and has the form given by equation (8). We trace from X_0 a ray segment that makes an angle β_0 with the surface normal at X_0 and has length equals to $v_0 t_0/2$. The extreme of that ray segment is the NIP. Do this for all central points that illuminate the first interface. Finally, we fit a cubic spline to the obtained NIPs, in a least-squares sense, to represent the interface. As a result of this process, the first layer is completely determined.

Subsequent layers. Let us assume that the model has been already determined up to the layer $(j-1)$. Note that this means that interface j has been already constructed. The input data are now the CRS parameters that refer to the zero-offset rays that reflect at the interface $(j+1)$. Trace the rays down to the interface j and back-propagate the NIP-wavefront along those rays. Applying the focusing conditions, estimate v_j by least squares. Using Snell's law calculate β_j and, knowing the remaining traveltimes, trace the last segment of each ray. To fit the many obtained NIPs an optimized cubic spline is estimated, representing, in this way, the interface $(j+1)$.

6 Synthetic examples

The algorithm was applied to the model depicted in Figure 7. That model consists of three interfaces separating four homogeneous layers. The second reflector has a synclinal region between 6.5km and 7.5km that generates caustics. The data was modeled by ray tracing, using the package Seis88 (Červený and Pšenčík (1984)). Noise was added to the data. The CRS parameters were estimated by the strategy described in Birgin et al. (1999). Finally, those parameters were inverted by the proposed method. The obtained model, depicted by solid bold lines in Figure 7, shows a very good agreement with the input model. It is to be noted that, for a fixed multicoverage data set, the illumination of the reflectors tend to be more confined for increasing depth. As a consequence, the apertures (horizontal extent) of the reconstructed interfaces will get increasingly smaller with depth. This effect can be readily observed in Figure 7.

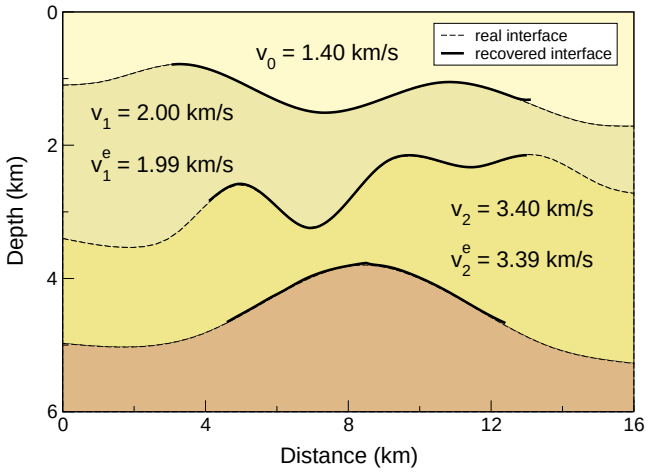

Figure 7: Synthetic model with four homogeneous layers separated by smooth interfaces (dashed lines). Inverted model composed by layers separated by the recovered interfaces (solid lines). v_j and v_j^e are the real and estimated velocities, respectively.

As a second example, we consider the model depicted in Figure 8(a). It is composed by four layers. The first and the fourth layers are homogeneous. The second and the third layers are inhomogeneous, in the sense that the velocity varies both in vertical and in horizontal directions. As before, the multicoverage data was modeled by ray tracing and noise was added to it. The estimated CRS parameters were inverted by the method. The result is the model depicted in Figure 8(b). Note that the resulting model has, of course vertical gradients. To better assess the accuracy of the recovered model, Figure 8(c) shows the percentual error between the synthetic and the inverted model. Note that the errors are, almost everywhere, below 5%. In fact, the Euclidean norm of the relative error is approximately 3.9.

7 Conclusions

The contribution of this work is an extension of the classical Hubral and Krey velocity-model inversion algorithm. That extension uses CRS parameters, obtained from previous application of the CRS stacking method. A significant improvement of the proposed algorithm is that it allows for (vertical) gradient velocity profiles inside each layer. The algorithm is also able to efficiently and accurately deal with caustic regions. Finally, the obtained interfaces are represented by optimized cubic splines, leading to very stable results. A discussion on the important aspects of the numerical implementation of the algorithm, as needed for an efficient application of the method, is provided. However, an investigation of the actual sensitivity of the algorithm to errors in the input data still needs to be done.

The algorithm retains the analytic layer-stripping character of the original Hubral and Krey approach, that is responsible for its good performance. This approach can very naturally complement more sophisticated global techniques such as seismic tomography, for example by producing useful initial models.

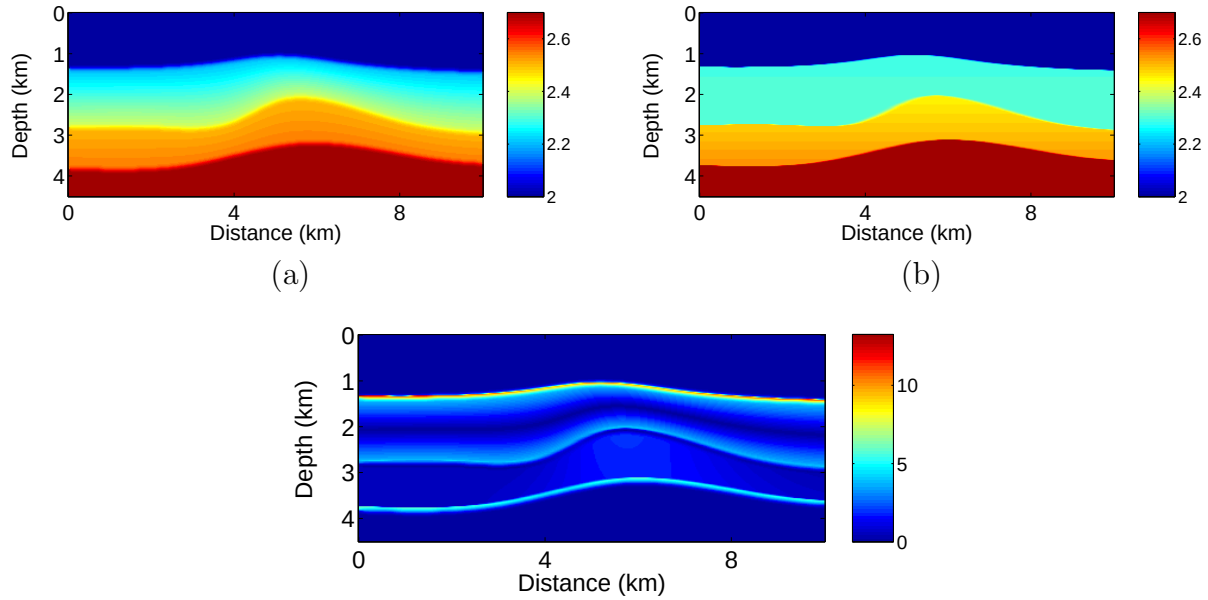

Figure 8: (a) Synthetic model with four layers, two homogeneous and two inhomogeneous. (b) Obtained model with gradients. (c) Percentual error, between the synthetic and the obtained model.

Two synthetic examples are shown, where the main features of the method can be illustrated. The results are encouraging. Concerning more complex velocity profiles, we may consider the application of algorithm on separated parts of the domain. Thus, each inverted model would be composed by layers with gradient-type velocity profiles that could, in a next step, be put together to form a complete inverted model. Research on these and other aspects of the algorithm are under current investigation.

8 Acknowledgements

This work was supported by FAPESP (Grant 97/12125-8) and CNPq, Brazil.

References

Berkovitch A.,and Gelchinsky, B., 1989. Inversion of common reflecting element (CRE) data. In *Expanded Abstracts of 59th Annual Internat. Mtg., Soc. of Expl. Geophys.*, pages 1250–1252.

Berkovitch, A., Gelchinsky, B., Keydar, S., and Shtivelman, V., 1991. Inversion of combined data of the CRE and CEE imaging. In *Expanded Abstracts of the 53th EAGE meeting*, pages 46– 47.

Biloti, R., 2001. *Multiparametric traveltimes: estimation and inversion*. PhD thesis, State University of Campinas, Brazil (in Portuguese).

Biloti, R., Santos, L. T., and Tygel, M., 2001. Layered velocity model from kinematic attributes. In *Extended Abstracts of the 7th International Congress of the Brazilian Geophysical Society*, pages 1055–1058, Salvador.

Birgin, E. G., Biloti, R., Tygel, M., and Santos, L. T., 1999. Restricted optimization: a clue to a fast and accurate implementation of the Common Reflection Surface stack method. *Journal of Applied Geophysics*, 42(3–4):143–155.

Birgin, E. G. and Martínez, J. M., 2001. Large-scale active-set box-constrained optimization method with spectral projected gradients. *Computational Optimization and Applications*, submitted.

Červený, V., 2001. *Seismic Ray Theory*. Cambridge University Press.

Červený, V. and Pšenčík, I., 1984. SEIS83 - numerical modeling of seismic wave fields in 2-D laterally varying structures by the ray method. *E. R. Engdahl (Ed.), Report SE-35*, pages 36–40.

Hubral, P., 1983. Computing true amplitude reflections in a laterally inhomogeneous earth. *Geophysics*, 48(8):1051–1062.

Hubral, P. and Krey, T., 1980. *Interval velocities from seismic reflection traveltime measurements*. Soc. Expl. Geophys.

Leite, L., 1998. *Introduction to spectral analysis in Geophysics*. FADESP, Belém, Brasil (in Portuguese).

Majer, P., 2000. Inversion of seismic parameters: Determination of the 2-D iso-velocity layer model. Master thesis, Karlsruhe University, Germany.

Müller, T., Jäger, R., and Höcht, G., 1998. Common reflection surface stacking method - imaging with an unknown velocity model. In *Expanded Abstracts of the 68th Ann. Internat. Mtg., Soc. of Expl. Geophys.*, pages 1764–1767.

Schleicher, J., Tygel, M., and Hubral, P., 1993. Parabolic and hyperbolic paraxial two-point traveltimes in 3D media. *Geophysical Prospecting*, 41:495–513.

Trappe, H., Gierse, G., and Pruessmann, J., 2001. Case studies show the potential of Common Reflection S urface stack - structural resolution in the time domain beyond the conventional NMO/DMO stack. *First Break*, 19(11):625–633.

Tygel, M., Müller, T., Hubral, P., and Schleicher, J., 1997. Eigenwave based multiparameter traveltime expansions. In *Expanded Abstracts of 67th Annual Internat. Mtg., Soc. of Expl. Geophys.*, volume 97, pages 1770–1773.

Vieth, K.-U., 2001. *Kinematic wavefield attributes in seismic imaging*. PhD thesis, Karlsruhe University, Germany.